POTENTIAL CLINICAL RELEVANCE

Nanomedicine: Nanotechnology, Biology, and Medicine
8 (2012) 1337–1344

Research Article

nanomedjournal.com

Nanoparticle-based adjuvant for enhanced protective efficacy of DNA vaccine Ag85A-ESAT-6-IL-21 against *Mycobacterium tuberculosis* infection

Fangliu Yu, PhD[a,1], Jing Wang, BS[b,1], Jun Dou, PhD[a,*,1], Haitao Yang, PhD[c], Xingfeng He, PhD[a], Weiguo Xu, BS[c], Yu Zhang, PhD[d], Kai Hu, PhD[a], Ning Gu, PhD[d]

[a]*Department of Pathogenic Biology and Immunology, Medical School, Southeast University, Nanjing, China*
[b]*Department of Gynecology and Obstetrics; Zhongda Hospital, Medical School, Southeast University, Nanjing, China*
[c]*Centers for Disease Control and Prevention of Jiangsu Province, Nanjing, China*
[d]*School of Biological Science and Medical Engineering, Southeast University, Nanjing, China*

Received 19 May 2011; accepted 27 February 2012

Abstract

The goal of this study was to evaluate the protective efficacy of a cationic nanoparticle-based DNA vaccine expressing antigen 85A (Ag85A) and 6-kDa early secretory antigen target (ESAT-6) of *Mycobacterium tuberculosis* as well as cytokine interleukin-21 (IL-21) against *M. tuberculosis* infection. The results of this indicated that the anti–*M. tuberculosis* immune responses were induced in mice that had received the different DNA vaccines. More importantly, compared with using DNA vaccine Ag85A-ESAT-6-IL-21 alone, the nanoparticle-based DNA vaccine Ag85A-ESAT-6-IL-21 showed a statistically significant increase in the protective efficacy against *M. tuberculosis* infection in the immunized mice. We concluded that the nanoparticle-based DNA vaccine induced a strong immune response and markedly inhibited the growth of the *M. tuberculosis* in the mice. These findings highlighted the potential utility of Fe_3O_4-Glu-polyethyleneimine nanoparticles encapsulated with the DNA vaccine as a prophylactic vaccine in the *M. tuberculosis*–infected mouse model.

From the Clinical Editor: This study emphasizes the potential utility of Fe_3O_4-Glu-polyethyleneimine nanoparticles encapsulated with DNA vaccine against TB as a prophylactic vaccine. The authors demonstrated a strong immune response and marked growth inhibition of mycobacterium tuberculosis in the mice.

Key words: *Mycobacterium tuberculosis*; Nanoparticles; Interleukin-21; DNA vaccine

Tuberculosis (TB), caused by *Mycobacterium tuberculosis*, is a worldwide public health problem that has affected humans for thousands of years. About one-third of the world population would have a positive skin test result for the infection and would be considered to be harboring *M. tuberculosis.*[1,2] The conventional anti-TB vaccine, *Mycobacterium bovis* bacille Calmette-Guérin (BCG), has been widely used to prevent TB since 1921. However, the protective efficacy of BCG has shown variable effects against adult pulmonary TB in different trials, even though it continues to be used to prevent meningitis and phthisis miliaris in children in many countries.[3-5] Because of the emergence of multidrug-resistant *M. tuberculosis* strains and human immunodeficiency virus infection, as well as the lack of success of the TB vaccine, there have been ongoing efforts to develop more effective vaccines using different strategies, such as the DNA vaccine and the protein vaccine, to combat TB.[1,6]

The DNA vaccine has emerged as a clinically viable and potentially safe vaccination strategy, and may have potential as a new vaccine for important pathogens such as TB, malaria, and hepatitis C.[7] Research has indicated that the TB DNA vaccine is a very powerful and easy method for inducing a strong immune response in mice. However, the clinical results of using the DNA vaccine have been disappointing with regard to the magnitude of induced immune responses.[8,9]

Interleukin-21 (IL-21) is involved in natural killer (NK) and T-cell activation; it has multiple immune functions, especially in

No conflict of interest was reported by the authors of this article.

This study was supported by grants of the Key Natural Science Foundation of Jiangsu Province, China (No.BK2007710), Novel project of Wuhu, China (No.2011 Public Health 7), and in part by the 973 Program of China (No.2011CB933500).

*Corresponding author: Department of Pathogenic Biology and Immunology, Medical School, Southeast University, No. 87 Ding Jiaqiao Road, Nanjing 210009, China.

E-mail address: njdoujun@yahoo.com.cn (J. Dou).

[1] These authors contributed equally to this work.

1549-9634/$ – see front matter © 2012 Elsevier Inc. All rights reserved.
http://dx.doi.org/10.1016/j.nano.2012.02.015

the tumor vaccine approaches.[10,11] IL-21 may serve as an immunostimulatory adjuvant for enhancing effector/memory lymphocyte responses in investigating the DNA vaccine that contains antigen 85A (Ag85A) of *M. tuberculosis* in the mouse model.[9,12] The 6-kDa early secretory antigen target (ESAT-6) is one of the most immunodominant and highly *M. tuberculosis*–specific target antigens, containing multiple immunogenic T-cell epitopes; therefore, it is capable of enhancing cell-mediated responses.[13] In previous studies, we developed a DNA vaccine expressing both a fusion protein of Ag85A-ESAT-6 and secreted IL-21 protein. The vaccine induced effective immune responses from the immunized mice, but the protection against *M. tuberculosis* challenge remained to be confirmed.[14]

In the present study we used nanoparticles (NPs) as delivery systems for the DNA vaccine Ag85A-ESAT-6-IL-21 to investigate its protective efficacy against *M. tuberculosis* challenge in the mouse model. Our data demonstrated that, compared with administration of the DNA vaccine Ag85A-ESAT-6-IL-21 alone, the NP-based DNA vaccine elicited a powerful immune response and significantly reduced the lung burden of *M. tuberculosis* in the vaccinated mice.

Methods

Materials

Animal and cell lines

Male C57BL/6 mice at 6 weeks of age were ordered from the Animal Center of Yang Zhou University of China and were raised at the Experimental Animal Center, Southeast University. All animal experiments were conducted following the guidelines of the Animal Research Ethics Board of Southeast University. Full details of the study approval can be found in the approval ID: 20080925. B16F10 murine melanoma cells are syngeneic in C57BL/6 mice, and YAC-1 cells (Moloney leukemia-induced T-cell lymphoma of A/Sn mouse origin) were obtained from the Cellular Institute of China in Shanghai. These cells were cultured in RPMI 1640 supplemented with 10% fetal bovine serum containing 100 units/mL penicillin G sodium and 100 μg/mL streptomycin sulfate.

M. tuberculosis, BCG, and DNA vaccine

M. tuberculosis H37Rv strain was grown in Sauton medium enriched with 0.5% (v/v) sodium pyruvate and 0.5% (v/v) glucose. BCG (Connaught strain; product ID: 2010080606) was a gift from the Centers for Disease Control and Prevention in Jiangsu Province of China. The DNA vaccine pIRES-IL-21-Ag85A-ESAT-6 was developed in our previous work.[9,14]

Engineering of PEI-NP–coated DNA vaccine pIRES-IL-21-Ag85A-ESAT-6

NPs of Fe_3O_4 coated with glutamic acid (nano-Fe_3O_4-Glu) were a gift from Dr. Chen Zhongping of Southeast University of China; these NPs have no cytotoxicity to cell lines in vitro.[15] Polyethyleneimine (PEI) was obtained from Sigma (Steinheim, Germany). The PEI-NP–coated DNA vaccine pIRES-IL-21-Ag85A-ESAT-6 or pIRES mock plasmid was prepared by vortexing the mixtures of 5 mL of the nano-Fe_3O_4-Glu to 1 mL PEI (5:1 ratio) for 60 minutes first, and then vortexing the mixtures with 2 μg/μL of DNA vaccine pIRES-IL-21-Ag85A-ESAT-6 or pIRES mock plasmid (2:1 ratio) for another 60 minutes.[16] The vaccine is a simple mixture, and an injection at the same site is necessary. The nano-Fe_3O_4-Glu particles were photographed under a scanning electron microscope. The zeta potential determination was based on the electrophoretic mobility of the NP-based DNA vaccine pIRES-IL-21-Ag85A-ESAT-6 in the aqueous medium by Zetasizer 3000 potentiometric analyzer, which was used to detect the surface potential of magnetic particles at different pH values (Malvern Instruments, Worcestershire, United Kingdom).

Transfections, reverse transcription–polymerase chain reaction, and western blot

B16F10 cells grown to 70% confluence were used in the transfection. Ten microliters of the NPs mixture suspensions that included the NPs and the DNA vaccine pIRES-IL-21-Ag85A-ESAT-6 were incubated with 1×10^6 B16F10 cells in six-well plates in medium for 4 hours at 37°C in 5% CO_2. The cells were washed with medium to remove the unbound NP mixtures and were incubated for a further 48 hours. As a reference, 1×10^6 B16F10 cells were transfected with 10 μg DNA vaccine pIRES-IL-21-Ag85A-ESAT-6 per well or 10 μg mock plasmid with Lipofectamine 2000 reagent (Invitrogen, Carlsbad, California) according to the manufacturer's instructions. Gene expressions were confirmed by western blot. Cells were collected and lysed in protein extraction buffer (Novagen, Madison, Wisconsin) according to the manufacturer's protocol. Western blotting was performed after 12% sodium dodecyl sulfate–polyacrylamide gel electrophoresis, and proteins (10 μg/lane) were electrotransferred onto a nitrocellulose membrane. The membrane was first blocked with blocking solution for 30 minutes and washed twice with water, and then incubated with goat antibody to Ag85A, goat antibody to ESAT-6, goat antibody to mouse IL-21 (I-18; Santa Cruz Biotechnology, Santa Cruz, California), and mouse antibody to GAPDH (Kangchen Company, Hangzhou City, China) for 1 hour, respectively. The subsequent steps were performed according to the Western-Breeze Kit protocol (Invitrogen).[6,17]

Immunization protocol and M. tuberculosis challenge

The mice for the study were randomly divided into seven groups as follows: group 1, phosphate buffered saline (PBS); group 2, pIRES mock plasmid; group 3, nano-Fe_3O_4-Glu mock plasmid; group 4, PAEI (mice received intramuscular injection of 100 μg DNA vaccine pIRES-Ag85A-ESAT-6-IL-21 in the right hind legs); group 5, Na-PAEI (mice received intramuscular injection of 50 μL of the PEI-NP–coated DNA vaccine suspensions in the right hind legs); group 6, BCG [mice received subcutaneous injections with 1×10^6 colony-forming units (CFU) of BCG][9]; group 7, no vaccination. Twenty-seven mice per group were used in groups 1 to 6. Nine mice were used in group 7. In the six vaccinated groups, each mouse was immunized three times with 3-week intervals between the immunizations. Two weeks after the final immunization, 9 mice from each of groups 1 to 6 were killed for detecting immune efficiency, and the remaining 18 mice in each group were used

for *M. tuberculosis* challenge. For the vaccine-protective experiment, each mouse was challenged through a lateral tail vein with 1×10^4 CFU of virulent *M. tuberculosis* H37Rv strain, diluted in 200 μL. Eight weeks after the challenge, nine mice from each of groups 1–7 were killed for detecting the bacterial burden, and the remaining nine mice from each of groups 1–6 were kept up to 24 weeks for obtaining murine weight.

Cytotoxic assays and splenocyte proliferation responses

The cytotoxic assays and splenocyte proliferation responses to Ag85A were, respectively, detected by a 3-(4,5-dimethylthiazol-2-yl)-2,5-diphenyltetrazolium bromide (MTT) assay.[6,18] For NK activity assay, 5×10^4 YAC-1 target cells were seeded in a 96-well plate with 2.5×10^6 effector cells at a 50:1 ratio of effector cells to target cells. After the plate was incubated for 20 hours and supernatant was discarded; 200 μL MTT were added to each well for an additional 4-hour incubation. The plates were measured with a plate reader (Bio-Rad Laboratories, Hercules, California) at OD_{490} after 20 μL dimethylsulfoxide was added. For $CD8^+$ splenocyte cytotoxicity, the assay was carried out as was described for NK activity assay. 2.5×10^6 splenocytes from the immunized mice were incubated with 5×10^4 B16F10 target cells transfected with pIRES-Ag85A-ESAT-6 or pIRES mock plasmid for 24 hours. $CD8^+$ splenocytes were isolated using magnetic microbeads (Miltenyi Biotec, CA).[19] For the splenocyte proliferation assay, 5×10^6 splenocytes were split in 96-well plates in the presence of 0.5 μg/mL Ag85A or in the absence of Ag85A. The results were expressed as stimulation index (SI). The cytotoxicities and SIs were calculated according to the previously reported methods.[6,9]

Antibody and cytokine detection by ELISA or ELISPOT

Sera were separated for detecting antibody to Ag85A (1:2000-fold dilution) or antibody ESAT-6 (1:1000-fold dilution) by the enzyme-linked immunosorbent assay (ELISA).[6] Interferon-γ (IFN-γ)-secreting cells were detected by ELISPOT assay (eBioscience Company, Bejing, China).[20] Samples and standards were run in triplicate.

Mycobacterial colony enumeration assay and histopathology

Eight weeks after the *M. tuberculosis* challenge the mice were killed and the right lungs were removed; the lungs from each group of mice were placed in 4 mL of PBS with 0.05% Tween 80, and homogenized with a tissue homogenizer. Two-hundred microliters of serially diluted homogenate were plated onto Middlebrook 7H10 agar plates (Becton-Dickinson, Franklin Lakes, New Jersey) containing 10% (v/v) oleic acid-albumin-dextrose-catalase enrichment and 0.5% glycerol (v/v) at 37°C for 16–20 days. The CFUs were counted under a dissection microscope.[19,21] The left lungs were fixed in 10% (v/v) neutral buffered formalin. Samples were removed by section of lung lobes that had been processed with paraffin wax. The sections were stained with hematoxylin and eosin for routine evaluation with Alizarin red to detect calcified lesions. The histopathological parameters peribronchiolitis, perivasculitis, alveolitis, and granuloma formation were each semiquantitatively scored as absent, minimal, slight, moderate, marked, or strong, denoted as 0, 1, 2, 3, 4, and 5, respectively. In this score both the frequency and the severity of the lesions were incorporated.[21]

Statistical analysis

Statistical analysis was performed using the Student's *t*-test for the difference between the experimental groups and control group. Bonferroni correction was used where multiple comparisons were made. The differences were considered as statistically significant when P values were less than 0.05.

Results

Nanoparticle morphology, zeta potential, protein expression, and influence of the NP DNA vaccine on B16F10 cells

Figure 1 shows transmission electron microscope (TEM) images of the NPs-Fe_3O_4-Glu (Figure 1, *A*), PEI-modified NP-Fe_3O_4-Glu (Figure 1, *B*), and DNA vaccine pIRES-IL-21-Ag85A-ESAT-6 modified by PEI-NP-Fe_3O_4-Glu (Figure 1, *C*). Figure 1, *D* indicates that the zeta potential of the NP-based DNA vaccine pIRES-Ag85A-ESAT-6-IL-21 was approximately +36 mV at neutral pH. The data suggest that, in pH 7.2–7.4 conditions, the zeta potential of the NP-based DNA vaccine matches the internal environment of host cells. The positive-charged particles formed may enhance the binding and internalizations to the cells, and may also offer the possibility of enhancement of their uptake by appropriate cells through manipulation of their surface properties.[22,23]

The expression of both the fusion protein of Ag85A-ESAT-6 and secreted IL-21 protein were confirmed by western blot, as is shown in Figure 1, *E*. These results suggested that the NP-based DNA vaccine pIRES-Ag85A-ESAT-6-IL-21 had been developed appropriately. The NPs modified by PEI with positively charged particles may be preferentially taken up by the cells as a result of the negative charge of the cellular membrane, and then the penetrating power of the NPs facilitated the process together with the DNA vaccine easily gaining cell entry.[1]

To evaluate the influence of the NP DNA vaccine on the cells, the proliferative behavior in the B16F10 cells transfected with the NP DNA vaccine in vitro was monitored by flow-cytometric analysis. S-phase fraction and proliferation index are two important parameters related to the cell cycle, and the parameters can actually reflect cellular proliferative states.[19] Figure 1, *F* and *G* exhibit the same proliferative behaviors in the B16F10 cells transfected with NP-based DNA vaccine as the untransfected B16F10 cells, because no significant correlation of S-phase fraction and proliferation index was found between the two cells. If the pDNA-NPs did inhibit proliferation of B16F10 cells, the NP-based DNA vaccine would inhibit proliferation of host cells when it was inoculated into mice; thus, it is not a reliable vaccine for the host cells. Therefore, our developed NP-based DNA vaccine would provide a feasible condition for further study of NP-based DNA vaccines in vivo.

M. tuberculosis challenge in vaccine-immunized mice

Table 1 shows that in these experiments significant protection against *M. tuberculosis* was achieved in all the mice immunized

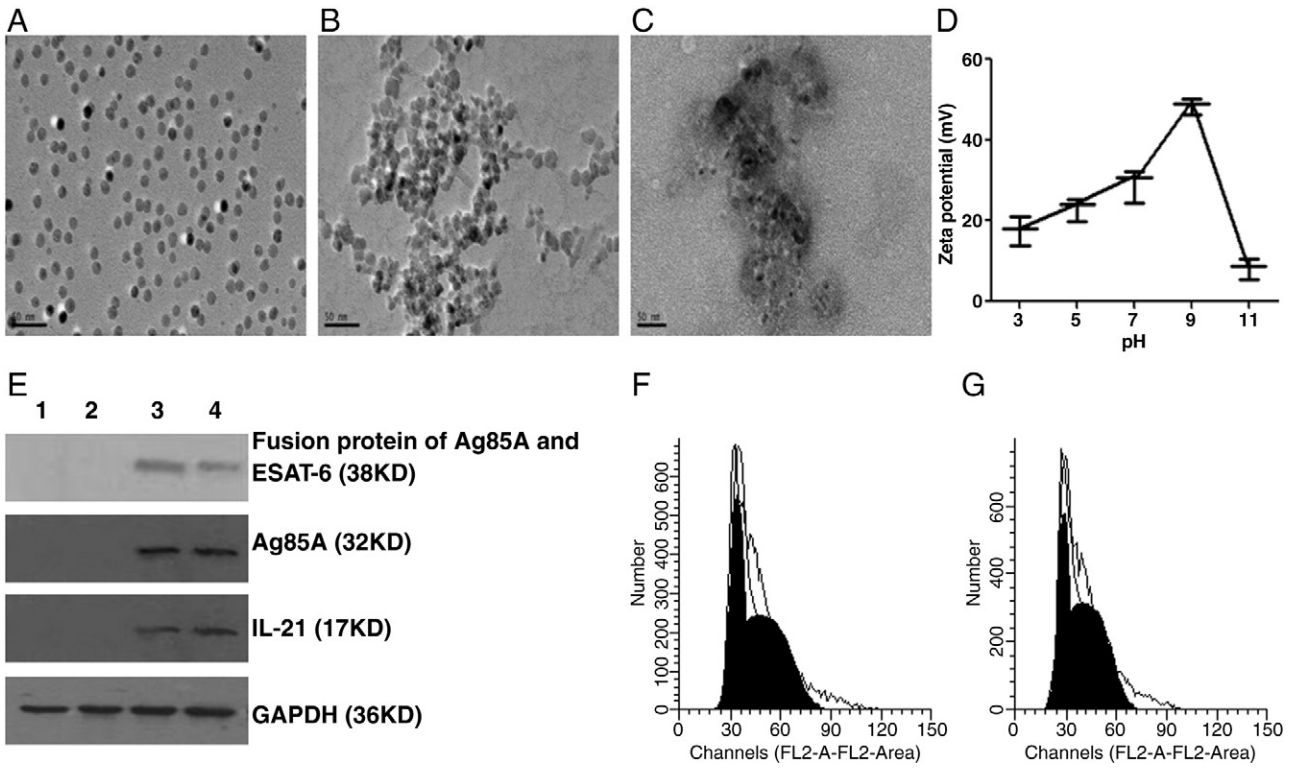

Figure 1. Images and zeta potential of the nano-Fe_3O_4-Glu NPs and protein expressions as well as influence of NP-based DNA vaccine on the B16F10 cell proliferation. **(A–C)** TEM images of **(A)** the nano-Fe_3O_4-Glu NPs, **(B)** PEI-modified nano-Fe_3O_4-Glu NPs, and **(C)** PEI-modified nano-Fe_3O_4-Glu NPs–coated DNA vaccine that were stained with uranyl acetate. Scale bar, 50 nm. **(D)** Zeta potential of the NPs-Fe_3O_4-Glu–coated DNA vaccine at different pH values. **(E)** Western blot. Lanes 1–4 show the results of protein expression in the B16F10 cells. Lane 1, B16F10 cells; lane 2, mock plasmid–transfected cells; lane 3, DNA vaccine pIRES-IL-21-Ag85A-ESAT-6–transfected cells in Lipofectamine, respectively; lane 4, the NP-based DNA vaccine–transfected cells. The fusion protein of Ag85A-ESAT-6 and secreted IL-21 protein were expressed correctly in their actual sizes in the transfected B16F10 cells. GAPDH was used as a control. There were no obvious changes of proliferative behaviors in the B16F10 cells transfected with the NP-based DNA vaccine **(F)** or without any transfection **(G)**.

with the different vaccines. However, the bacterial growth was significantly inhibited in the NP-based DNA vaccine group, with a 57-fold decrease in the total number of CFU (4.42 ± 0.64 vs. 6.18 ± 0.67, $P < 0.001$) in the NP-based DNA vaccine group (Na-PAEI) compared with the DNA vaccine pIRES-Ag85A-ESAT-6-IL-21 (PAEI) group; a 10-fold decrease in CFU (4.42 ± 0.64 vs. 5.45 ± 0.68, $P < 0.001$) compared with the BCG group; and a 457-fold decrease in CFU (4.42 ± 0.64 vs. 7.08 ± 0.74, $P < 0.001$) compared with the PBS group. The net weight in the immunized mice was also a good indicator; the data suggested that the NP-based DNA vaccine was an efficient prevention against infection by *M. tuberculosis*, with the vaccine's powerful capability to reduce the bacterial burdens in the mouse lungs and to increase the murine net weight after being challenged with *M. tuberculosis*.

Histopathological analysis

The lung injury was effectively lessened in the mice immunized with the NP-based DNA vaccine, and the well-contained small granulomas (Figure 2, *E*, *arrows*) exhibited general infiltration of numerous lymphocytes and neutrophils. The pathological changes with BCG vaccination (Figure 2, *F*) were similar to those in Figure 2, *E*. Less alveolar architecture was present in the BCG-vaccinated mice. Figure 2, *D* shows a slight inflammation response and some caseation necrosis with moderate lymphocytic infiltration in the mice immunized with the DNA vaccine pIRES-Ag85A-ESAT-6-IL-21 alone, which showed slightly greater injury than that of mice vaccinated with the NP-based DNA vaccine. The pathological changes were serious in the mice immunized with the PBS (Figure 2, *A*), the mock plasmid (Figure 2, *B*), and the NP-based mock plasmid (Figure 2, *C*). Figure 2, *A–C* show less-contained granulomas and many more infiltrated inflammation cells as well as TB lesions. Figure 2, *G* shows the normal alveolar architecture. Figure 2, *H* presents the different semiquantitative scores of lung pathological changes.

Cell-mediated immunity

The results for the cytotoxicities of NK cells, splenocytes, and $CD8^+$ splenocytes are shown in Figure 3, *A* and *B*. The NK cytotoxicity of the NP-based DNA vaccine group was the highest (53.26 ± 5.17%) among the six groups. The BCG group ranked second (47.64 ± 4.92%), followed by the pIRES-Ag85A-ESAT-6-IL-21 group (43.64 ± 4.10%). The NK cytotoxicities were less than 20.00% in the other three groups. There were statistically significant differences between the NP-based DNA vaccine

Table 1
Vaccine-induced protection against *M. tuberculosis* challenge

Groups	Log_{10}CFU	Weight (g)		
		Pre-infect.	Post-infect.	Net Weight
PBS	7.08±0.74	21.08±0.36	21.75±0.40	0.67±0.33
PIRES	7.02±0.62	20.91±0.37	21.61±0.61	0.70±0.41
Na-P	6.94±0.52	21.00±0.33	21.59±0.33	0.59±0.34
PAEI	6.18±0.67	21.18±0.42	22.44±0.47	1.26±0.14
Na-PAEI	4.42±0.64	21.11±0.35	23.63±0.58	2.28±0.39
BCG	5.45±0.68	21.02±0.32	22.75±0.47	1.73±0.44

CFU, colony-forming unit; PBS, phosphate buffered saline group; pIRES, pIRES mock plasmid group; Na-P, pIRES mock plasmid + NP group; PAEI, pIRES-IL-21-Ag85A-ESAT-6 (DNA alone) group; Na-PAEI, pIRES-IL-21-Ag85A-ESAT-6 + NP group; BCG, bacille Calmette-Guérin group. Bacterial burdens were calculated from nine mice per group per experiment for two experiments, and weights were calculated from nine mice per group for two experiments. Bacterial data and weight data do not come from the same mice, and data from multiple experiments were pooled for calculations and statistics. Asterisks (∗) show statistically significant differences between two groups as judged by Student's *t*-test and Bonferroni correction followed where multiple comparison tests were done (**P* < 0.05; ***P* < 0.03; ****P* < 0.01).

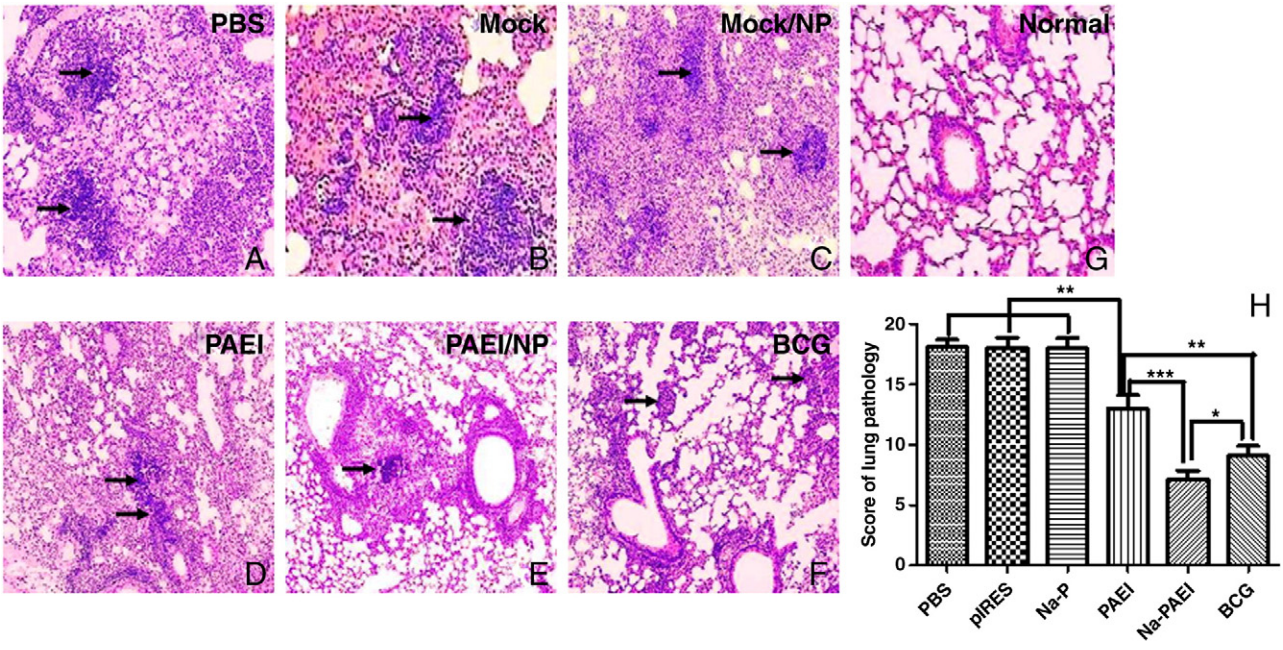

Figure 2. Lung histopathological changes in the mice immunized with the vaccines (hematoxylin and eosin staining, magnification, ×100). **(A–F)** All representative pathological changes in the immunized mice in **(A)** the PBS group, **(B)** the mock plasmid group, **(C)** the mock plasmid + NPs group, **(D)** the PAEI group, **(E)** the PAEI + NPs group, and **(F)** the BCG group. **(G)** Normal alveolar architecture without any infection. **(H)** Results of the semiquantitative analysis of histopathological changes. Each histogram represents a set of data for nine mice. **P* < 0.05; ***P* < 0.03; ****P* < 0.01.

group and the pIRES-Ag85A-ESAT-6-IL-21 group or the BCG group ($P < 0.05$), as is shown in Figure 3, *A*. Higher cytotoxicities in the splenocytes and $CD8^+$splenocytes were induced by the NP-based DNA vaccine than in the pIRES-Ag85A-ESAT-6-IL-21 ($P < 0.05$) and the BCG group ($P < 0.05$), or than that of the other three groups ($P < 0.01$), respectively, as is shown in Figure 3, *B*.

The splenocyte proliferative response to Ag85A was significantly increased in the mice immunized with the NP-based DNA vaccine compared with the pIRES-Ag85A-ESAT-6-IL-21 group ($P < 0.05$) or the BCG group ($P < 0.05$), and the other three groups ($P < 0.01$), as is shown in Figure 3, *C*. The SI in the NP-based DNA vaccine group was the highest among the six groups; the BCG group ranked second, followed by the pIRES-Ag85A-ESAT-6-IL-21group. The SI was less than 0.50 in the other three groups. These results suggested that the NP-based DNA vaccine induced a high cytotoxicity and vigorous splenocyte proliferative response to Ag85A. However, the

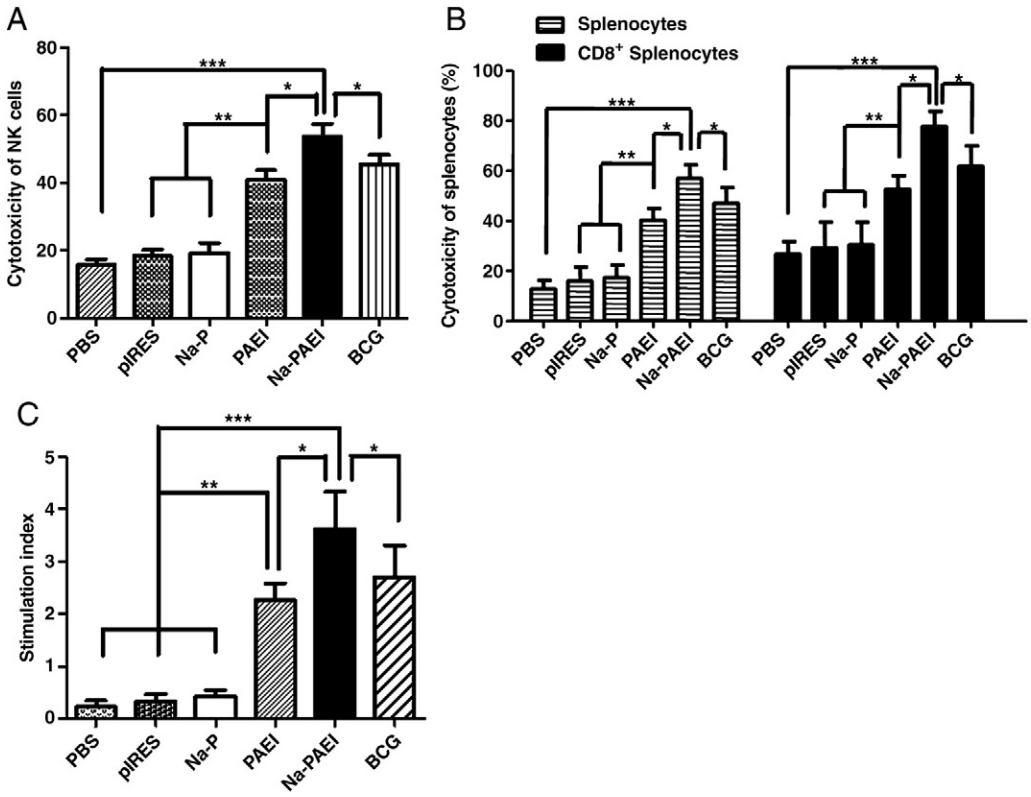

Figure 3. Cytotoxicities and splenocyte proliferative responses to the various treatments. **(A, B)** Cytotoxicity percent of **(A)** NK cells, and of **(B)** splenocytes and $CD8^+$ splenocytes, respectively. **(C)** Splenocyte proliferative responses to Ag85A. Each bar in the histogram represents a different group as shown on the *x*-axis. $*P < 0.05$, $**P < 0.03$, $***P < 0.01$.

specificity of these responses has not yet been studied, because we did not detect the specificity for either antigen (Ag85A, ESAT-6).

Detection of antibody responses and cytokine in the vaccinated mice

Figure 4, *A* shows that the levels of serum anti-ESAT-6 and anti-Ag85A in mice immunized with the NP-based DNA vaccine were significantly increased compared with the levels in the DNA vaccine pIRES-Ag85A-ESAT-6-IL-21 group ($P < 0.05$) and the BCG group ($P < 0.03$ with antibody to Ag85A, and $P < 0.01$ with antibody to ESAT-6), and the other three groups ($P < 0.001$), respectively. Figure 4, *B* shows that the background level was lower than 10 spot-secreting cells (SSCs) per 10^5 lymphocytes in the PBS, pIRES, and Na-P groups, but the numbers of SSCs reached as many as 162 to 174 per 10^5 cells in mice immunized with the NP-based DNA vaccine. These results suggested that the NP-based DNA vaccine pIRES-Ag85A-ESAT-6-IL-21 could elicit specific antibody responses to ESAT-6 and Ag85A as well as a high number of IFN-γ SSCs in the immunized mice.

Discussion

The development of NP-based delivery systems for improved TB vaccines has been shown to be an exciting emerging field.[1,22-24] It has been reported that the DNA vaccine encoding Ag85A was adsorbed by cationic poly(D,L-lactide-*co*-glycolide) (PLGA) microparticles, which indicated that the vaccine has strong protective efficacy against *M. tuberculosis* challenge in mice.[23] The immunogenicity of the DNA vaccine encoding the *M. tuberculosis* latency antigen Rv1733c and co-formulation with PLGA-PEI NPs on host immunity were explored using a DNA prime–protein boost vaccination regimen in mice.[25] These studies of the NP-based DNA vaccines against *M. tuberculosis* represent one promising approach.

In this study we developed the DNA vaccine Ag85A-ESAT-6-IL-21–coated nano- Fe_3O_4-Glu, in which the IL-21 acted as the immunostimulatory adjuvant co-expressing with target antigens of Ag85A-ESAT-6, and the nano-Fe_3O_4-Glu served as the delivery system. Furthermore, we evaluated the immunogenicity of the DNA vaccine and its protective efficacy against the *M. tuberculosis* challenge in a mouse model. The results showed that the NP-based DNA vaccine was effectively transported into the B16F10 cells. The proteins Ag85A-ESAT-6 and IL-21 were expressed correctly, and the transfection efficiency of DNA vaccine using NPs was the same as that of the DNA vaccine Ag85A-ESAT-6-IL-21 using Lipofectamine. The findings suggested that the barrier to transporting plasmid DNA through cell membrane was overcome by our prepared NPs.[26,27] This was further verified by the experimental results that an immunogenicity and the protective efficacy of DNA vaccine Ag85A-ESAT-6-IL-21–coated cationic NPs against

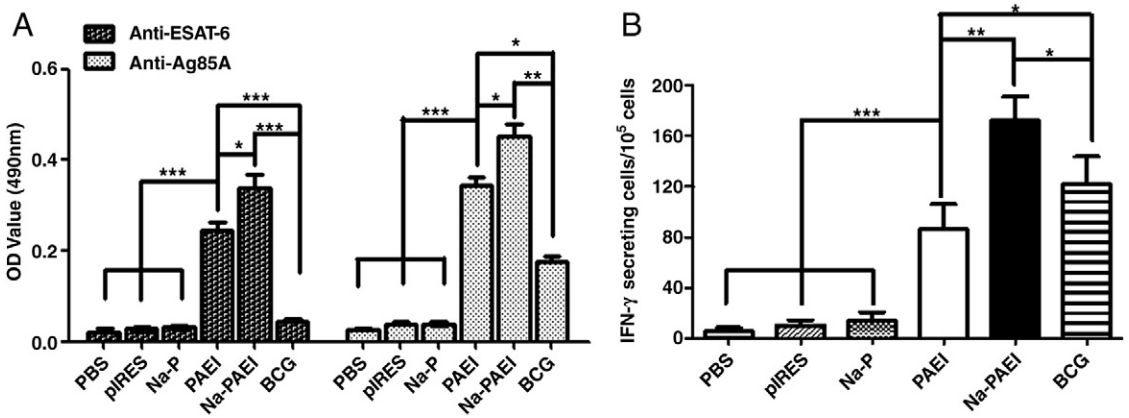

Figure 4. Levels of antibody and cytokine. **(A)** Serum levels of antibody to ESAT-6 and antibody to Ag85A in the vaccinated mice. **(B)** Numbers of spot-secreting cells (i.e., secreting IFN-γ) per 10^5lymphocytes in the vaccinated mice. PBS, pIRES, Na-P, PAEI, Na-PAEI, and BCG are described as in Figure 2. The histograms represent the levels of antibody and cytokine for nine mice. $*P < 0.05$, $**P < 0.03$, $***P < 0.01$.

M. tuberculosis infection were significantly increased in the vaccinated mice.

Our findings also demonstrated that the NP-based DNA vaccine expressing fusion protein of Ag85A-ESAT-6 and secreted IL-21 protein could induce *M. tuberculosis*–specific immune responses that were capable of obviously enhancing the antibody levels and the number of IFN-γ SSCs (IL-4 SSCs was much fewer; data not shown). The cytotoxicities of the NK cells, splenocytes, and $CD8^+$ splenocytes as well as splenocyte proliferative responses to Ag85A were respectively enhanced. More significantly, the specific immune responses resulted in remarkable protective efficacy against *M. tuberculosis* challenge, which was reflected in markedly inhibiting the lung injury and the increase in mouse net weight after the *M. tuberculosis* challenge. Although the DNA vaccine Ag85A-ESAT-6-IL-21 and BCG also elicited an effective immune response and protective efficacy against *M. tuberculosis* challenge, the efficacy was greater in the mice vaccinated with the NP-based DNA vaccine. To our knowledge, this is the first demonstration that the DNA vaccine Ag85A-ESAT-6-IL-21 coated with Fe_3O_4-Glu-PEI NPs induced more powerful immune responses and much more protective efficacy against the *M. tuberculosis* challenge in mice. These findings highlighted the potential utility of Fe_3O_4-Glu-PEI NPs co-encapsulated with DNA vaccine as the prophylactic vaccine in the *M. tuberculosis*–infected mouse model.

We think that the possible mechanism for the developed DNA vaccine is that IL-21 stimulates the production of IFN-γ, which enhances the presentation of the fusion protein of Ag85A-ESAT-6 to lymphocytes by dendritic cells. IFN-γ also elicits T-lymphocyte immune responses to Ag85A-ESAT-6,[9,22] and generates more IFN-γ expression by NK cells.[28,29] From the results of the cytotoxicity tests, especially in the cytotoxicity of $CD8^+$ splenocytes, we think that the $CD8^+$ lymphocytes may perform a key function in protecting mice against *M. tuberculosis* infections. Another potential mechanism is that the developed DNA vaccine can be co-encapsulated with nano-Fe_3O_4-Glu, which may act as a depot for the slow release of antigens, resulting in the activation of immune responses, and in the prolonged immune responses for augmentation of immune efficacy.[30,31]

Conclusions

Collectively, our results demonstrated that the improved DNA vaccine Ag85A-ESAT-6-IL-21–coated Fe_3O_4 NPs transported plasmid DNA vaccine into cells effectively and induced powerful immune responses and protection against *M. tuberculosis* challenge in contrast to using the DNA vaccine Ag85A-ESAT-6-IL-21 alone in a mouse model. Our findings therefore call for approaches that might enhance the immune prophylactic efficacy using a novel cationic NP-based DNA vaccine delivery system to prevent pulmonary TB.

References

1. Griffiths G, Nyström B, Stable SB, Khuller GK. Nanobead-based interventions for the treatment and prevention of tuberculosis. *Nat Rev Microbiol* 2010;**8**:827-34.
2. Russell DG, Rarry CE, Flynn JL. Tuberculosis: what we don't know can, and does, hurt us. *Science* 2010;**328**:852-6.
3. Espinal MA, Laszlo A, Simonsen L. Global trends in resistance to antituberculosis drugs. World Health Organization–International Union against tuberculosis and lung disease working group on anti-tuberculosis drug resistance surveillance. *N Engl J Med* 2001;**344**: 1203-14.
4. Claire SA, Jes D, Else MA, Lycke NY, Lövgren K, Andersen P. The combined CTA1-DD/ISCOMs vector is an effective intranasal adjuvant for boosting prior *Mycobacterium bovis* BCG immunity to *Mycobacterium tuberculosis*. *Infect Immun* 2007;**75**:408-16.
5. Kaufmann SH, McMichael AJ. Annulling a dangerous liaison: vaccination strategies against AIDS and tuberculosis. *Nat Med* 2005; **11**:S33-44.
6. Jun D , Quan T, Fangliu Y, Haitao Y, Fengshu Z, Weiguo X, et al. Investigation of immunogenic effect of the BCG priming and Ag85AGM-CSF boosting in Balb/c mice model. *Immunobiology* 2010;**215**:133-42.
7. Huygen K. DNA vaccines against mycobacterial diseases. *Future Microbiol* 2006;**1**:63-73.

8. Mumper RJ, Cui Z. Genetic immunization by jet injection of targeted pDNA-coated nanoparticles. *Methods* 2003;**31**:255-62.
9. Jun D, Quan T, Fengshu Z, Lili C, Junsong C, Minggang C, et al. Comparison of immune responses induced in mice by vaccination with DNA vaccine constructs expressing mycobacterial antigen 85A and interleukin-21 and Bacillus Galmette-Guérin. *Immunol Invest* 2008; **37**:113-27.
10. Parrish NJ, Dillon SR, Nelson A, Hammond A, Sprecher C, Gross JA. Interleukin 21 and its receptor are involved in NK cell expansion and regulation of lymphocyte function. *Nature* 2000;**408**:57-63.
11. Dou J, Wu Y, Wang J, Zhao F, Chu L, Liu C, et al. Eliciting protective immune responses against murine myeloma challenge in lymphopenia mice through adoptive transfer of tumor antigen-specific lymphocytes and immunization of tumor vaccine secreting mIL-21. *Cancer Gene Therapy* 2010;**17**:675-83.
12. Kim SS, Kim HS, Fan Q, Kim DW, Kaufman HL. Local IL-21 promotes the therapeutic activity of effector T cells by decreasing regulatory T cells within the tumor microenvironment. *Mol Ther* 2009;**17**:380-8.
13. Millington KA, Fortune SM, Low J, Garces A, Hingley-Wilson SM, Wickremasinghe M, et al. Rv3615c is a highly immunodominant RD1 (Region of Difference 1)-dependent secreted antigen specific for *Mycobacterium tuberculosis* infection. *Proc Natl Acad Sci U S A* 2011; **108**:5730-5.
14. Jinlong L, Fangliu Y, Jun D. Constructing nucleic acid vaccine expressing fusion antigens of *Mycobacterium tuberculosis* Ag85A and ESAT-6, and Interleukin 21 as well as studying its immune effect in mice. *Lett Biotechnol* 2009;**20**:800-3.
15. Ma M, Zhu Y, Zhang Y, Zhang D, Tang Z, Zhang H, et al. Preparation of magnetite nanoparticles and interaction with cancer cells. *J Southeast Univ (Natural Sci Edn)* 2003;**3**:205-7.
16. Kai H, Jun D, Fangliu Y, Xiangfeng H, Xianwen Y, Yaqing W, et al. An ocular mucosal administration of nanocarriers containing DNA vaccine pRSC-gD-IL-21 confers protection against mucosal challenge with herpes simplex virus type 1 in mice. *Vaccine* 2011;**29**:1455-62.
17. Dou J, Liu P, Wang J, Zhang X. Effect of hepatitis C virus core shadow protein expressed in human hepatoma cell line on human gene expression profiles. *J Gastroenterol Hepatol* 2006;**21**:1794-800.
18. Mosmann TR. Colorimetric assay for cellular growth and survival: application to proliferation and cytotoxicity assays. *J Immunol Methods* 1983;**65**:55-63.
19. Zhao F, Dou J, He X, Wang J, Chu L, Hu W, et al. Enhancing therapy of B16F10 melanoma efficacy through tumor vaccine expressing GPI-anchored IL-21 and secreting GM-CSF in mouse model. *Vaccine* 2010;**28**:2846-52.
20. Clark SO, Kelly DL, Badell E, Castello-Branco LR, Aldwell F, Winter N, et al. Oral delivery of BCG Moreau Rio de Janeiro gives equivalent protection against tuberculosis but with reduced pathology compared to parenteral BCG Danish vaccination. *Vaccine* 2010;**28**: 7109-16.
21. Dormans J, Burger M, Aguilar D, Hernandez-Pando R, Kremer K, Roholl P, et al. Correlation of1 virulence, lung pathology, bacterial load and delayed type hypersensitivity responses after infection with different *Mycobacterium tuberculosis* genotypes in a BALB/c mouse model. *Clin Exp Immunol* 2004;**137**:460-8.
22. Clawson C, Huang CT, Futalan D, Martin SD, Saenz R, Larsson M, et al. Delivery of a peptide via poly (D,L-lactic-*co*-glycolic) acid nanoparticles enhances its dendritic cell-stimulatory capacity. *Nanomed Nanotechnol Biol Med* 2010;**6**:651-61.
23. Bivas-Benita M, Lin MY, Bal SM, van Meijgaarden KE, Franken KL, Friggen AH, et al. Pulmonary delivery of DNA encoding *Mycobacterium tuberculosis* latency antigen Rv1733c associated to PLGA-PEI nanoparticles enhances T cell responses in a DNA prime/protein boost vaccination regimen in mice. *Vaccine* 2009;**27**:4010-7.
24. Singh M, Chakrapani A, O'Hagan D. Nanoparticles and microparticles as vaccine-delivery systems. *Expert Rev Vaccine* 2007;**6**:797-808.
25. Couvreur P, Vauthier C. Nanotechnology: intelligent design to treat complex disease. *Pharm Res* 2006;**23**:1417-50.
26. Lawson LB, Freytag LC, Clements JD. Use of nanocarriers for transdermal vaccine delivery. *Clin Pharmacol Ther* 2007;**82**:641-3.
27. Lyadova IV, Vordermeier HM, Eruslanov EB, Khaidukov SV, Apt AS, Hewinson RG. Intranasal BCG vaccination protects BALB/c mice against virulent *Mycobacterium bovis* and accelerates production of IFN-γ in their lungs. *Clin Exp Immunol* 2001;**126**:274-9.
28. Cooper AM. Cell-mediated immune responses in tuberculosis. *Annu Rev Immunol* 2005;**27**:393-422.
29. Cui Z, Mumper RJ. The effect of co-administration of adjuvants with a nanoparticle-based genetic vaccine delivery system on the resulting immune responses. *Eur J Pharm Biopharm* 2003;**55**:11-8.
30. Zaman M, Skwarczynski M, Malcolm JM, Urbani CN, Jia Z, Batzloff MR, et al. Self-adjuvanting polyacrylic nanoparticulate delivery system for group A streptococcus (GAS) vaccine. *Nanomed Nanotechnol Biol Med* 2011;**7**:168-73.
31. Naeem K, Donna B, Rachel B, Nayak L, Rickinson AB, Moss PA. T cell recognition patterns of immunodominant cytomegalovirus antigens in primary and persistent infection. *J Immunol* 2007;**178**:4455-65.